

## Review paper

Preparation and characterization of sintered ceramics made  
with spent foundry olivine sand and clayE. Furlani <sup>\*</sup>, G. Tonello, E. Aneggi, S. Maschio*Università di Udine, Dipartimento di Chimica, Fisica e Ambiente, Via del Cotonificio 108, 33100 Udine, Italy*

Received 12 September 2011; received in revised form 23 November 2011; accepted 25 November 2011

Available online 4 December 2011

**Abstract**

Two different types of clay (a yellow and a red clay) were used to prepare two sets of materials containing spent foundry olivine sand. They were blended by attrition milling in varying proportions to obtain powders of different composition.

All mixtures were dried, sieved, uniaxially pressed into specimens and air sintered for 1 h at temperatures ranging from 900 to 1140 °C. The resulting materials were characterized by density, water absorption, shrinkage, crystallographic composition, microstructure and physico-mechanical properties. Mechanical and crystallographic properties were determined on samples fired at 1040 °C in order to compare materials with similar characteristics. It was observed that, after sintering, all compositions show the presence of the glassy phase which surrounds the crystalline grains and the set of materials prepared using the red clay displayed best overall behavior. XRD analysis performed on the free surface of the fired samples did not show the presence of compounds containing heavy metals present in the starting materials.

© 2011 Elsevier Ltd and Techna Group S.r.l. All rights reserved.

**Keywords:** A. Sintering; C. Mechanical properties; D. Clays; Foundry sand

**Contents**

1. Introduction . . . . .	2619
2. Materials and methods . . . . .	2620
3. Results and discussion . . . . .	2621
4. Conclusions. . . . .	2624
References . . . . .	2624

**1. Introduction**

Spent foundry sand (FS) is a by-product of the metal-casting industries which use sand in their moulding and casting operations. Moulds can be used many times, but after a certain number of cycles, the sand inconsistent with the casting, is generally disposed of in landfill.

For the production of one ton of cast material, between 75 and 150 kg of moulding sand [1] is also produced; it follows

that spent sand is considered one of the major problems of the foundries [2].

End life foundry sands often contain a mixture of silica sand, olivine sand, bentonite clay, coal dust and water; their dark color (almost black) is due to the carbonaceous components which derive from thermal decomposition of organic compounds used in order to agglomerate the green sand and enable to create a reducing atmosphere during casting [3].

Spent foundry sands also contain small fractions of heavy metals and, before any landfill disposal, they must be stabilized with calcium hydroxide [4,5] in order to limit any possible elution process which could release hazardous elements into the environment. This practice has a high cost, is not an optimal eco-solution and has induced many authors to propose alternative options such as: production of special concretes

<sup>\*</sup> Corresponding author. Tel.: +39 432 558877; fax: +39 432 558803.

E-mail addresses: [erika.furlani@uniud.it](mailto:erika.furlani@uniud.it) (E. Furlani),  
[gabriele.tonello@uniud.it](mailto:gabriele.tonello@uniud.it) (G. Tonello), [eleonora.aneggi@uniud.it](mailto:eleonora.aneggi@uniud.it) (E. Aneggi),  
[stef.maschio@uniud.it](mailto:stef.maschio@uniud.it) (S. Maschio).

[6–10], component of flowable fills [11,12] and production of clay bricks [5]. If the attention is focused to the field of ceramics, it can be observed that quartz is a raw material used for the production of several traditional products, however just few papers dealing with spent silica foundry sand recycling have been recently published [5]; conversely, the use of olivine is limited to the production of some refractory bricks [13,14] or particular glaze for tiles [15] and the use of spent foundry olivine sand is not documented at all.

The use of waste materials in the ceramic industry has been proposed by several authors [16–19], since this option permits to couple a double function: (i) production of new marketable tools and (ii) inertization of the many hazardous components of the waste into a stable silicatic network. It is known in fact that silica based glassy or crystalline highly dense materials are leach resistant and can help to preserve environment from hazardous elements contamination [20–23].

The aim of present research is to evaluate a possible use of spent FS mixed, in different proportions, with a natural clay for the production of some ceramic materials. Two different clays were used and each one was mixed with 10, 20 and 40 wt.% of spent FS. Pure clay samples were also prepared, tested and used as blank references.

Powders of each composition, pressed into several specimens, were fired at different temperatures for 1 h, then shrinkage and water absorption were measured in order build up their sintering curves. Apparent density, microstructure, crystal phases and some mechanical properties were tested in a second time on product fired at 1040 °C.

## 2. Materials and methods

The FS used in the present work is an end-life mainly olivine sand used as moulding material in a foundry process devoted to the production of a high manganese steel; it was dried in an oven for 24 h at 80 °C and then transformed into a coarse powder by a mortar; natural clays used to balance the mixtures are a yellow clay (YC) and a red clay (RC). The composition of the above raw materials, obtained by a Spectro Mass 2000 Induced Coupled Plasma (ICP) mass spectrometer, is reported in Table 1 which also displays lost on ignition (LOI) data obtained after a thermal treatment at 1000 °C for 2 h. With the used analytical method, the made error is below 3% of each determination.

Table 2 displays the composition of the samples prepared and the abbreviations used to define each material.

Blends (70 g of powder for each preparation) were homogenized by attrition milling for 1 h in a homemade instrument. Milling parameters are as follows: high-density

Table 2

Composition of the samples prepared and abbreviations used for materials identification along the paper (RC, red clay; YC, yellow clay; FS, foundry sand).

Material name	R	RS1	RS2	RS4	Y	YS1	YS2	YS4
RC (wt.%)	100	90	80	60	–	–	–	–
YC (wt.%)	–	–	–	–	100	90	80	60
FS (wt.%)	–	10	20	40	–	10	20	40

nylon container (volume = 750 ml); 500 g of 99 wt.% alumina balls (diameters = 6–8 mm); 150 ml of distilled water; 300 cycles min<sup>−1</sup>. Slurries were then oven dried for 24 h at 80 °C. After milling, particle size distribution (PSD) was evaluated using a Horiba LA950 laser scattering particle size distribution analyzer: analyses were made in water after a 3 min sonication time. For clarity of comprehension PSD curves are represented with logarithmic abscissa, as it is commonly done for the presentation of this type of results. Dried powders were sieved (200 µm ~70 mesh) and uniaxially pressed at 100 MPa into parallelepipedal specimens (5 mm × 5 mm × 50 mm). Density of green samples was determined by the ratio between weight and volume which was evaluated by a caliper. Reported data are averaged over three measurements. Sintering experiments were performed in air, by an electric muffle, at several temperatures ranging from 900 to 1140 °C with intervals of 20 °C using heating and cooling rates of 10 °C/min and a D-well time of 1 h.

Shrinkage on firing was evaluated, by a caliper, along the longest samples dimension (50 mm on green specimens) using the ratio  $(h_0 - h_1)/h_0$  (subscripts 0 and 1 refer to the sample dimensions before and after the sintering). Apparent density of sintered materials was determined by the Archimedes method whereas water absorption was determined following the norm EN99; in line with this norm, fired samples were first weighed in air ( $W_1$ ), then placed in a covered beaker and boiled in water for 2 h. After boiling, samples were cooled in water to room temperature, dried with a cloth and weighed again ( $W_2$ ). Water absorption was evaluated using the formula:  $W (\%) = 100 [(W_2 - W_1)/W_1]$ . In all the above measurements data variation remains below 10% of the averaged value.

Crystal phases, microstructures, apparent density, bend rupture strength and Vickers hardness were measured only on specimens fired at 1040 °C since it was observed that only after such firing cycle, all compositions had comparable overall characteristics.

Crystal phases were investigated by X-ray diffraction (XRD); XRD patterns were recorded on a Philips X'Pert diffractometer operated at 40 kV and 40 mA using Ni-filtered Cu-K $\alpha$  radiation. Spectra were collected using a step size of

Table 1

Chemical composition (wt.%) and LOI (%) of red clay (RC), yellow clay (YC) and that of foundry sand (FS) reported in term of major oxides.

Comp	SiO <sub>2</sub>	Al <sub>2</sub> O <sub>3</sub>	CaO	MgO	Na <sub>2</sub> O	K <sub>2</sub> O	Fe <sub>2</sub> O <sub>3</sub>	TiO <sub>2</sub>	P <sub>2</sub> O <sub>5</sub>	NiO	Cr <sub>2</sub> O <sub>3</sub>	MoO <sub>2</sub>	Undet	LOI
RC	42.67	27.93	2.87	2.24	1.35	3.84	7.15	0.52	0.11	–	–	–	1.37	9.95
YC	48.36	24.57	1.99	1.18	1.25	5.34	4.13	0.62	0.10	–	–	–	1.25	11.21
FS	55.10	1.89	5.25	8.85	0.41	0.74	4.76	0.16	0.25	1.15	1.40	0.66	1.38	18.00

0.02° and a counting time of 15 s per angular abscissa in the range 5–80°. The Philips X'Pert HighScore software was used for phase identification.

Density was evaluated by the Archimedes method, flexural rupture strength ( $\sigma$ ) was evaluated by the 4-point bending test with a crosshead speed of 0.2 mm min<sup>-1</sup> using a Shimadzu AG10 equipment whereas Vickers hardness ( $H_v$ ) was determined by a 100 N load with a Zwick indenter on polished surfaces (6  $\mu$ m diamond paste); data herein reported are all averaged over 10 measurements. Microstructures were examined, on the as fired materials, by an Assing Stereoscan scanning electron microscope (SEM).

### 3. Results and discussion

The chemical analysis revealed that RC and YC have similar chemical compositions, the main difference being the amount of iron oxide which, in RC, is greater than YC; the presence of high quantities of SiO<sub>2</sub>, Al<sub>2</sub>O<sub>3</sub> and minor fractions of other components are in line with literature data [24–26]. FS contains high quantities of SiO<sub>2</sub>, MgO, CaO and Fe<sub>2</sub>O<sub>3</sub> and moderate amounts of Al<sub>2</sub>O<sub>3</sub>, NiO, Cr<sub>2</sub>O<sub>3</sub> whereas other oxides can be considered minor components. The LOI of the two clays is in line with literature data [25,26], whereas that of FS is higher thus revealing the presence of a large content of organic matter or free carbon in the as received material.

Unlike the chemical analysis, the X-rays diffraction investigation (Fig. 1) revealed some differences between the crystal phases of RC and YC. In fact, it was identified the presence of quartz (PDF 01-083-2465) and kaolinite (PDF 00-029-1488) in each clay, but RC contains also dolomite (PDF 00-036-0426) and other phases which were not clearly identified due to the low intensity and limited number of the corresponding diffraction peaks and therefore not reported. However there is a clear peak around 9° 2theta which could mean 30–50% illite and would turn the two clays into illite–kaolinite type, i.e. the most common ceramic clays. On the other hand, FS displayed an XRD pattern showing a great amount of quartz, olivine (PDF 00-003-0195), calcite (PDF 01-086-2339) and a compound of the pyroxene's family namely calcium magnesium iron aluminum silicate (PDF 00-050-1544).

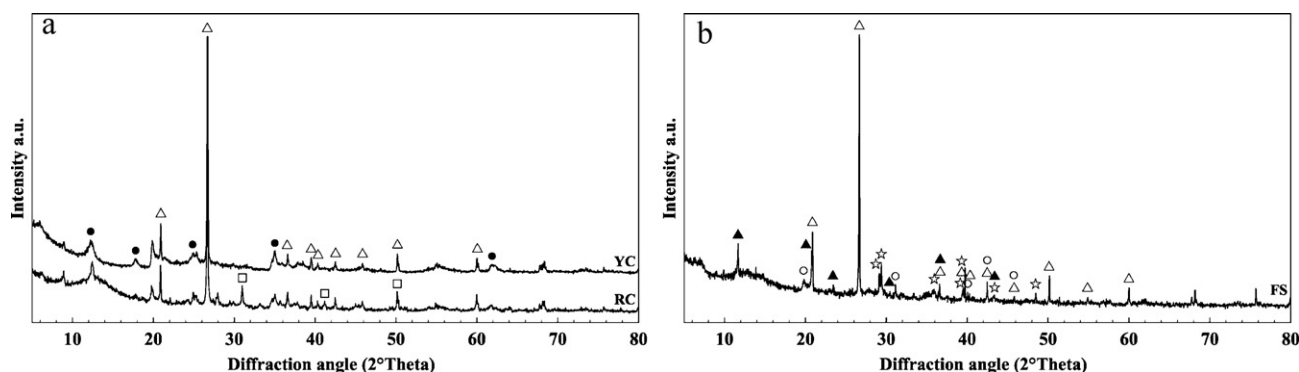


Fig. 1. X-ray diffraction patterns (5–80°) of as received RC, YC (a) and FS (b). Phases can be identified as follows: ( $\Delta$ ) quartz; ( $\bullet$ ) kaolinite; ( $\square$ ) dolomite; ( $\circ$ ) olivine; ( $\blacktriangle$ ) calcium magnesium iron aluminum silicate and ( $\star$ ) calcite.

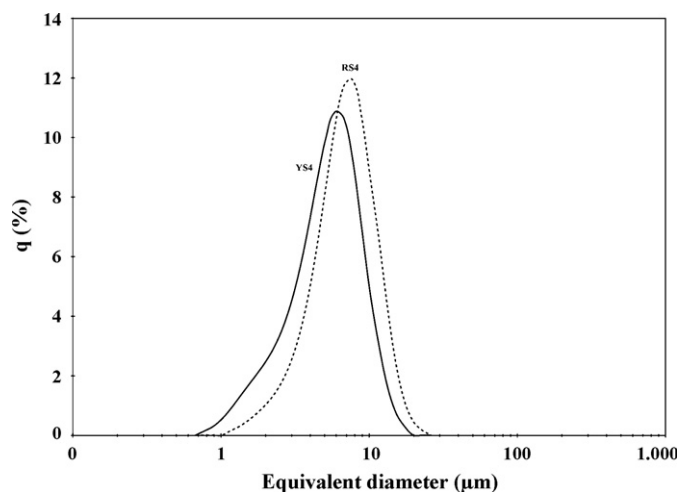


Fig. 2. Particle size distribution of the milled powders with compositions YS4 and RS4. Curves are represented with logarithmic abscissa.

Fig. 2 shows the PSD curves, determined after the milling procedure, relative to powders blends of composition RS4 and YS4. It can be observed that both curves display a monomodal particle size distribution with the maximum at around 6  $\mu$ m (YS4) and 7.5  $\mu$ m (RS4) respectively; it can be also observed that both powders do not contain particles exceeding the size of 30  $\mu$ m. All the other compositions showed similar monomodal particles size distribution, with the maximum in the range 5–9  $\mu$ m. As a consequence of the milling procedure, it was assumed to neglect the effect of powders PSD on the properties of the resulting sintered materials.

Water absorption, directly related to the open porosity, and linear shrinkage are physical parameters used for drawing the sintering curves which lead to optimization of firing cycles and, in turn, to the production of materials with optimized properties. It must be however pointed out that water absorption is not porosity, but related to the open porosity.

Fig. 3a and b reports shrinkage trends as a function of the firing temperature of all the compositions. It has been observed that the addition of FS causes the formation of a great amount of liquid phase in materials fired at temperature greater than 1120 °C. As a consequence, samples with such compositions loose their shape and shrinkage cannot be determined. It has

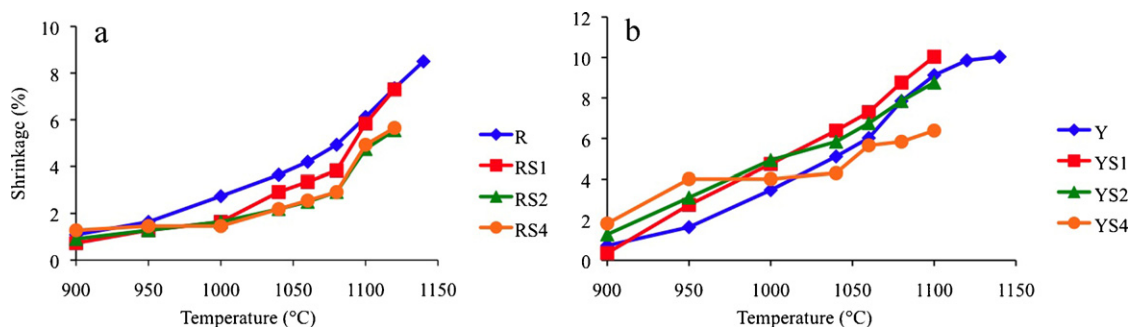


Fig. 3. Shrinkage (%) as a function of the firing temperature of the materials containing RC (a) or YC (b).

been seen (Fig. 3a) that materials prepared using RC alone show a growing monotonic trend up to 1140 °C. The addition of waste sand to the clay causes a shrinkage reduction, with respect to the pure clay, in the whole range 900–1120 °C.

Also among materials containing YC (Fig. 3b), it has been observed that compositions YS1, YS2 and YS4 soften between 1100 and 1120 °C, probably due to a partial melting of some phases, and in this set of samples it was not possible to measure the shrinkage at temperatures higher than 1100 °C; the only Y alone was therefore tested in the whole range established. In this context, it is seen that composition Y, YS1 and YS2 display a monotonic growing shrinkage trend, being that of YS1 and YS2 greater than that of the Y alone thus showing that the addition of FS to the clay improves shrinkage. On the other hand, composition YS4 shows a flat trend between 950 and 1040 °C whereas before and after this interval a growing trend is observed.

It must be pointed out that all compositions fired at temperatures below 1040 °C show shrinkage values below 6.5% and therefore could be considered suitable for the industrial production of some typologies of commercial ceramic materials [27].

Fig. 4a and b reports water absorption vs. firing temperature of the materials produced. Concerning the set of materials containing RC, it has been observed that R alone shows a continuous decreasing trend in the whole range examined, being 8% after a thermal treatment at 900 °C and around zero after firing at 1120 °C or higher temperatures. Conversely, RS1, RS2 and RS4 reveal increasing values between 900 and 1060 °C then a rapid decrease of water absorption data can be observed. Such behavior is reasonably due to the formation of

liquid phase which is associated to the raising of bubbles before materials completely loose their original shape [28–30]. It must be also pointed out that, after a thermal treatment at 1120 °C, RS1 and RS2 reach values close to zero, whereas water absorption of RS4 remains greater than 6.0%. This particular behavior probably depends on the great amount of carbon in the FS which, in turn, causes relevant residual open porosity which cannot be closed by material's shrinkage. As expected, also the behavior of materials containing YC depends of the amount of FS added: Y, YS1 and YS2 show a continuous bland decrease of water absorption as a function of the final firing temperature; on the other hand, YS4 shows an almost flat trend in the range 950–1040 °C and then it slowly decreases up to 1100 °C which is the typical behavior observed in several blends of powders used for the production of tiles and in agreement with the trend observed by other authors who proposed the use of waste materials in the production of ceramic tiles [31–36].

One should also keep in mind that water absorption, shrinkage and then bending strength values are interdependent, so that to the lower water absorption corresponds to the greater linear shrinkage and then high bending strength. In this respect, it is worth pointing out that water absorption values below 10% meet the official Italian requirements for the production of commercial ceramic materials therefore it can be concluded that, if other parameters are not considered, many compositions prepared in the present research are in line with the norm, provided that products could be fired at their optimal sintering temperature.

Fig. 5 shows the X-ray diffraction patterns of the samples made with RC and YC fired at 1040 °C; this temperature was selected in order to test materials with a completely developed

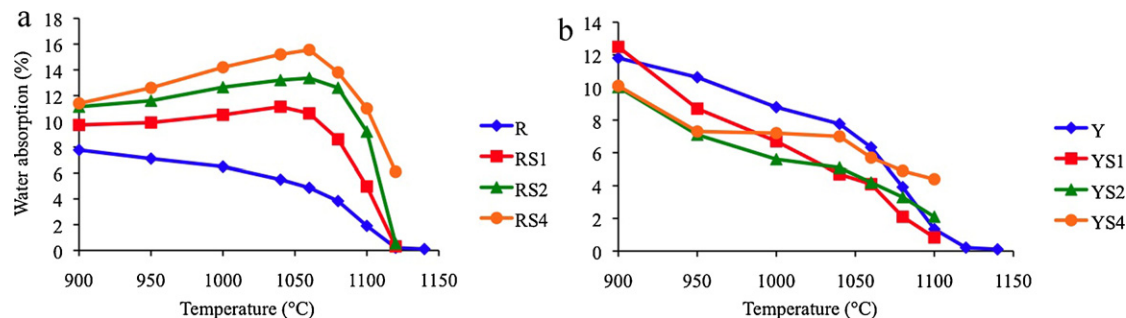


Fig. 4. Water absorption (%) vs. sintering temperature of the samples prepared using RC (a) or YC (b).



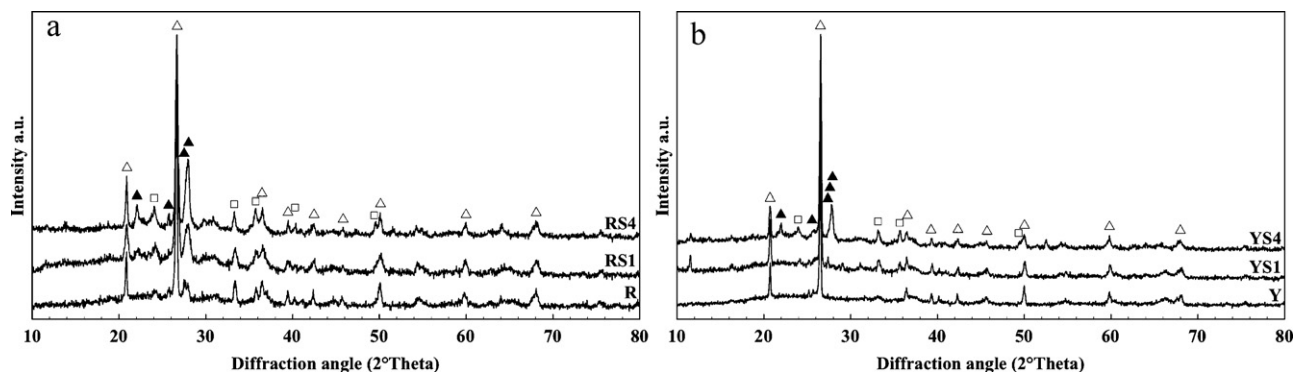


Fig. 5. X-ray diffraction patterns (10–80°) of the as fired surface of the samples with composition R, RS1, RS4 (a) and Y, YS1, YS4 (b). Phases are identified as: (Δ) quartz; (□) hematite and (▲) anorthite.

crystalline structure and a limited quantity of vitreous phase as a result of a firing cycle sufficiently far from the softening temperature of each composition.

The phases detected in materials fired at 1040 °C are consistent with those revealed in the raw materials. It can be observed that samples made with the two clays alone mainly contain residual quartz that is already present in the starting

clay which in the case of R is accompanied by small fractions of two anorthite like phases namely albite (PDF 01-083-1613) and orthoclase (PDF 01-083-1253) and hematite (PDF 01-085-0987) whose amount increases with the added quantity of FS. On the other hand the addition of FS to YC favor the crystallization of anorthite and hematite which were not detected in samples made with YC alone. Due to the low intensity and limited number of the corresponding diffraction peaks, other phases were not clearly identified. All patterns also showed a not flat profile of the background line thus revealing the presence of a not negligible quantity of vitreous phase. It must be also pointed out that the XRD analysis did not reveal the presence of free heavy metals oxides (i.e. Cr<sub>2</sub>O<sub>3</sub>, MoO<sub>3</sub>, NiO) nor Mg containing crystal phases. Since such elements are present in the starting materials, but they were not detected in the fired samples it is possible to speculate their sequestration by the vitreous phase or contained into the two anorthite-like feldspar structures, namely albite and orthoclase.

This result, also supports the different behaviors observed in the sintering curves. It can be concluded that the crystal structure of the fired materials at 1040 °C is mainly determined by nature, chemical composition and crystal phases of the natural materials used and minimally by the chemistry of the recycled material (FS).

The presence of vitreous phase in all the samples fired at 1040 °C or above was confirmed by the SEM analysis and it is documented by Figs. 6a and b and 7a and b which show 4 micrographs of the as fired (1040 °C) surfaces of the samples with compositions R, RS4, Y and YS4; other micrographs were considered not necessary and, in order to limit redundant documentation, are not reported in the present paper.

It can be observed that, together with a residual open porosity compatible with the one determined by the water absorption tests, all samples contain a relevant amount of glass material (the presence of polycrystalline grains has been already documented by the XRD analysis), but SEM micrographs also show that the vitreous phase is widely diffused and covers all grains by a layer of glass.

The presence of cracks caused by the β-quartz to α-quartz transition was not observed probably due to the small size of quartz grains (see Fig. 2) and to the relatively low cooling rate during the sintering process [37,38].

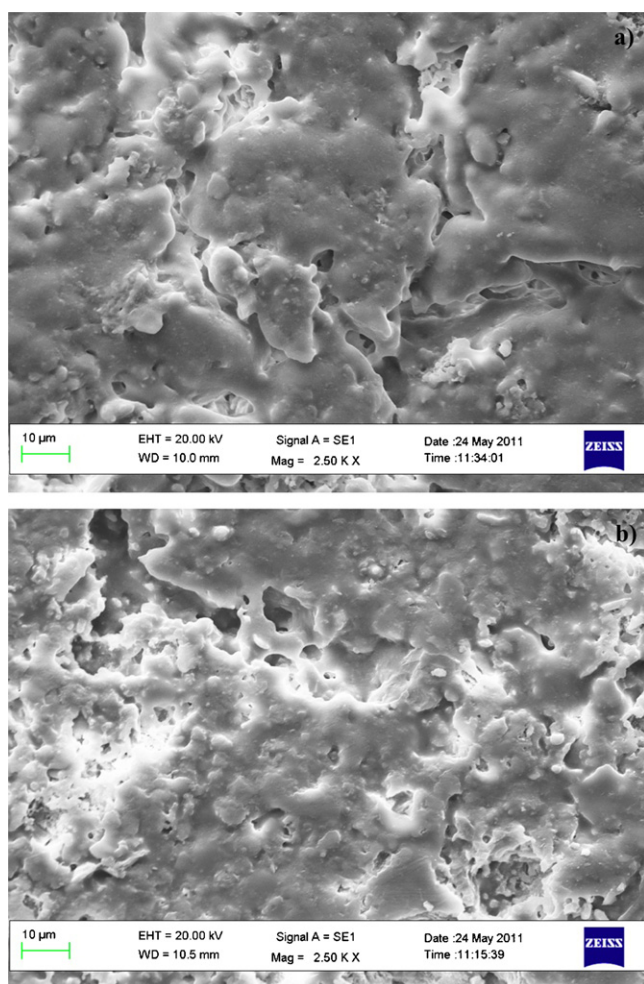


Fig. 6. SEM micrograph showing the free surface of the sintered R (a) and RS4 (b).

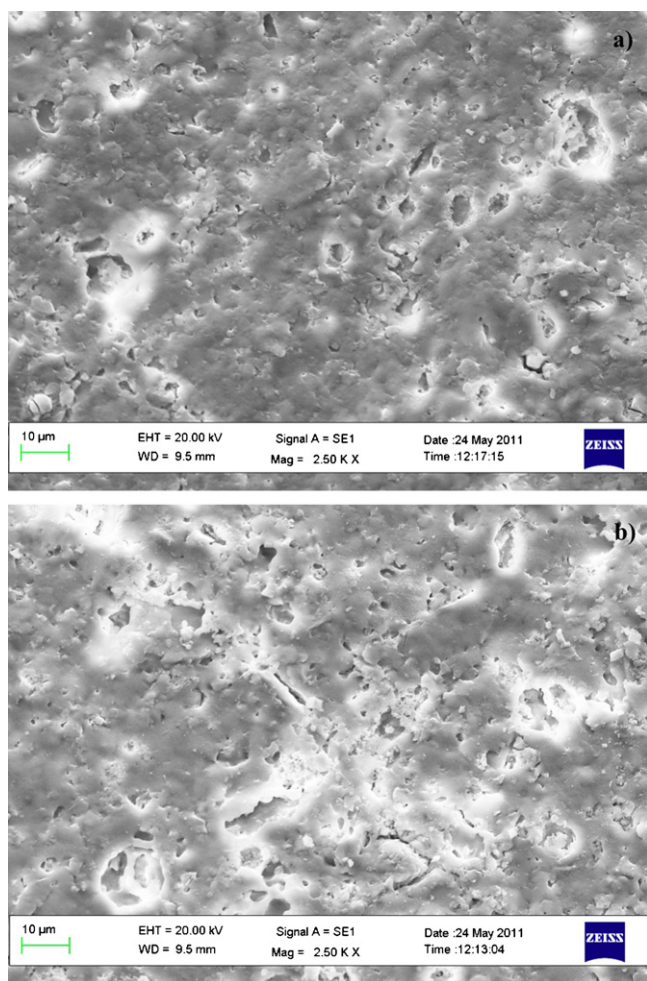


Fig. 7. SEM micrograph showing the free surface of the sintered Y (a) and YS4 (b).

Table 3 reports apparent density of green and fired materials, flexural rupture strength and Vickers hardness of the samples fired at 1040 °C for 1 h. Density of green specimens decreases as the amount of FS is increased reasonably due to the high amount of carbonaceous compounds there contained. It is known that density values determined as described in Section 2 are affected by errors of 10% or even more.

Strength and hardness variability of each composition is limited being always below 15% of the average value and seems to be not affected by materials composition. At the same time, all the properties are in agreement with water absorption, i.e. when water absorption is low, also density, strength and hardness are high and vice versa. It can be also observed that the presence of different phases seems to have little influence on materials properties, their values being probably much more dependent on composition and properties of the vitreous phase. The low apparent density of composition RS4 is in conflict with shrinkage data. This is reasonably due to two synergistic effects: the most important, makes longitudinal sample shrinkage positive, but transversal shrinkage negative and is due to the presence of bulk bubbles raised together with the liquid phase as previously discussed. The other is caused by the presence of unburned carbon, introduced with FS, which

Table 3

Averaged values of apparent density ( $\rho$ ) of green and fired materials, flexural rupture strength ( $\sigma$ ) and Vickers hardness ( $H_v$ ) of samples fired at 1040 °C; variability is also displayed.

Material's name	$\rho_{\text{green}}$ [g/cm <sup>3</sup> ]	$\rho_{\text{fired}}$ [g/cm <sup>3</sup> ]	$\sigma$ [MPa]	$H_v$ [GPa]
R	2.20	2.42	43 ± 3	4.2 ± 0.2
RS1	2.05	2.10	33 ± 4	3.8 ± 0.3
RS2	2.00	2.05	28 ± 3	3.5 ± 0.2
RS4	2.00	1.85	24 ± 4	3.0 ± 0.2
Y	2.15	2.30	38 ± 2	3.9 ± 0.5
YS1	2.15	2.25	49 ± 3	4.4 ± 0.3
YS2	2.10	2.20	43 ± 4	4.2 ± 0.2
YS4	2.10	2.20	39 ± 3	4.0 ± 0.4

partially transforms into entrapped gaseous products during sintering and partially causes a wide black core in samples with this composition as highlighted by samples fracture surface after the bend strength tests. Such coupled effects also determine limited mechanical performances. All the other compositions showed mechanical performances in line with literature data for materials produced using recycled waste [39–42] and the presence of black core was not observed.

#### 4. Conclusions

The present research deals with production and characterization of ceramics prepared using two natural clays alone or blended with 10, 20 and 40 wt.% of one spent foundry sand. The sintering experiments demonstrated that:

- the crystal structure of the fired materials is mainly due to nature, chemical composition and crystal phases of the natural clay and minimally by the characteristics of the FS;
- the XRD analysis detected some phases already present in the starting components;
- XRD analysis of the fired samples did not show the presence of compounds containing heavy metals;
- the SEM investigation showed that polycrystalline grains are covered by a layer of glass thus confirming the presence of the vitreous phase; and
- the mechanical performances of the different blends is dependent on their water absorption values and therefore on their residual open porosity, nevertheless in composition named RS4 it was observed the presence of black core after the rupture test of the samples and therefore revealing the presence, in this only composition, of entrapped unburned carbon.

#### References

- [1] M.C. Zanetti, S. Fiore, Foundry processes: the recovery of green moulding sands for core operations, *Res. Conserv. Recy.* 38 (2002) 243–254.
- [2] European Commission, Integrated pollution prevention and control. Reference document on best available techniques in the smitheries and foundries industry, May 2005.
- [3] R.S. Dungan, N.H. Dees, The characterization of total and leachable metals in foundry moulding sands, *J. Environ. Manage.* 90 (2009) 539–548.

- [4] A. Coz, A. Andrés, S. Soriano, A. Irabien, Environmental behaviour of stabilized foundry sludge, *J. Hazard. Mater. B* 109 (1–3) (2001) 95–104.
- [5] R. Alonso-Santurde, A. Andrès, J.R. Viguri, M. Raimondo, G. Guarini, C. Zanelli, M. Dondi, Technological behaviour and recycling potential of spent foundry sands, *J. Environ. Manage.* 92 (2011) 994–1002.
- [6] R.N. Kraus, T.R. Naik, B.W. Ramme, R. Kumar, Use of foundry silica-dust in manufacturing economical self-consolidating concrete, *Constr. Build. Mater.* 23 (2009) 3439–3442.
- [7] R. Siddique, G. de Schutter, A. Noumowe, Effect of used-foundry sand on the mechanical properties of concrete, *Constr. Build. Mater.* 23 (2009) 976–980.
- [8] Y. Guney, Y.D. Sari, M. Yalcin, A. Tuncan, S. Donmez, Re-usage of waste foundry sand in high-strength concrete, *Waste Manage.* 30 (2010) 1705–1713.
- [9] S. Fiore, M.C. Zanetti, Foundry wastes reuse and recycling in concrete production, *Am. J. Environ. Sci.* 3 (2007) 135–142.
- [10] R. Siddique, A. Noumowe, Utilization of spent foundry sand in controlled low-strength materials and concrete, *Res. Conserv. Recy.* 53 (2008) 27–35.
- [11] Y. Guney, A.H. Aydilek, M.M. Demirkan, Geoenvironmental behaviour of foundry sand amended mixtures for highway subbases, *Waste Manage.* 26 (2006) 932–945.
- [12] A. Deng, P.J. Tikalsky, Geotechnical and leaching properties of flowable fill incorporating waste foundry sand, *Waste Manage.* 28 (2008) 2161–2170.
- [13] H. Palmour III, B. Gay, R.L. Cochrane, Olivine refractory bricks for heat storage applications, US Patent no. 4,303,448 (1981).
- [14] V.M. Goldschmidt, Olivine and forsterite refractories in Europe, *Ind. Eng. Chem.* 30 (1938) 32–34.
- [15] M. Schabbach, F. Andreola, I. Lancellotti, L. Barbieri, Minimization of Pb content in a ceramic glaze by reformulation the composition with secondary raw materials, *Ceram. Int.* 37 (2011) 1367–1375.
- [16] F. Andreola, L. Barbieri, E. Karamanova, I. Lancellotti, M. Pelino, Recycling of CRT panel glass as fluxing agent in the porcelain stoneware tile production, *Ceram. Int.* 34 (2008) 1289–1295.
- [17] V.K. Marghussian, A. Magsoodipoor, Fabrication of unglazed floor tiles containing Iranian copper slag, *Ceram. Int.* 25 (1999) 617.
- [18] A. Selinger, V. Schmidt, Investigation of sintering processes in bottom ash to promote the reuse in civil construction, parts 1 & 2, in: G.R. Woolley, J.J.J.M. Goumans, P.J. Wainwright (Eds.), *Waste Materials in Construction: Putting Theory into Practice*, Elsevier, Amsterdam, 1997, pp. 41–58.
- [19] C. Fiori, A. Brusa, Iron slags containing body for the production of wall tiles by a rapid single firing techniques, *Ceram. Powd.* (1983) 161–172, Elsevier, New York.
- [20] C.R. Cheeseman, S. Monteiro da Rocha, C. Sollars, S. Bethanis, A.R. Boccaccini, Ceramic processing of incinerator bottom ash, *Waste Manage.* 23 (10) (2003) 907–916.
- [21] S. Maschio, E. Furlani, S. Bruckner, D. Minichelli, Synthesis and characterization of ceramics from coal fly ash and incinerated paper mill sludge, *Ceram. Int.* 34 (2008) 2137–2142.
- [22] E. Furlani, G. Tonello, S. Maschio, E. Aneggi, S. Bruckner, D. Minichelli, E. Lucchini, Sintering and characterization of ceramics containing paper sludge, glass cullet and different types of clayey materials, *Ceram. Int.* 37 (2011) 1293–1299.
- [23] M. Romero, J.M. Rincón, R.D. Rawlings, A.R. Boccaccini, Use of vitrified urban incinerator waste as raw material for production of sintered glass–ceramics, *Mater. Res. Bull.* 36 (2001) 383–395.
- [24] M. Dondi, Clay materials for ceramic tiles from the Sassuolo District Northern Apennines, Italy. Geology, composition and technological properties, *Appl. Clay Sci.* 15 (1999) 337–366.
- [25] B. Strazzera, M. Dondi, M. Marsigli, Composition and ceramic properties of tertiary clays from southern Sardinia (Italy), *Appl. Clay Sci.* 12 (1997) 247–266.
- [26] S.K. Das, K. Dana, N. Singh, R. Sarkar, Shrinkage and strength behaviour of quartzitic and kaolinitic clays in wall tile compositions, *Appl. Clay Sci.* 29 (2005) 137–143.
- [27] T. Manfredini, G.C. Pellacani, *Engineering materials handbook, Ceramics and Glasses – ASTM 925-929*, vol. 4, 1992.
- [28] R.W. Grimshaw, *The Chemistry and Physics of Clays and Allied Ceramic Materials*, Ernest Benn Ltd., London, 1971.
- [29] F.H. Norton, *Elements of Ceramics*, Addison-Wesley Press, Cambridge, 1952.
- [30] A. Cassan, D. Goi, F. Tubaro, S. Brückner, A. Bachiarrini, S. Maschio, Sintering behaviour of thermally treated municipal sewage sludge (MSS), *Ind. Ceram.* 24 (3) (2004) 173–179.
- [31] M.S. Hernandez-Crespo, J.M. Rincon, New porcelainized stoneware materials obtained by recycling of MSW incinerator fly ashes and granite sawing residues, *Ceram. Int.* 27 (2001) 713–720.
- [32] F. Andreola, L. Barbieri, A. Corradi, I. Lancellotti, T. Manfredini, Utilisation of municipal incinerator grate slag for manufacturing porcelainized stoneware tiles manufacturing, *J. Eur. Ceram. Soc.* 22 (2002) 1457–1462.
- [33] J. Martin-Marquez, J.M. Rincon, M. Romero, Effect of firing temperature on sintering of porcelain stoneware tiles, *Ceram. Int.* 34 (2008) 1867–1873.
- [34] S. Ferrari, A.F. Gualtieri, The use of illitic clays in the production of stoneware tile ceramics, *Appl. Clay Sci.* 32 (2006) 73–81.
- [35] C.M.F. Vieira, R. Sanchez, S.N. Monteiro, Characteristics of clays and properties of building ceramics in the state of Rio de Janeiro, Brazil, *Constr. Build. Mat.* 22 (2008) 781–787.
- [36] I. Ozdemir, S. Yilmaz, Processing of unglazed ceramic tiles from blast furnace slag, *J. Mater. Process. Technol.* 183 (2007) 13–17.
- [37] F.M. Wahl, R.E. Grim, R.B. Graf, Phase transformations in silice as examined by continuous X-ray diffraction, *Am. Mineral.* 46 (1961) 196–207.
- [38] A. De Noni Jr., D. Hotza, V. Cantavella Soler, E. Sanchez Vilches, Effect of quartz particle size on the mechanical behaviour of porcelain tiles subjected to different cooling rates, *J. Eur. Ceram. Soc.* 29 (2009) 1039–1046.
- [39] A.R. Boccaccini, M. Petitmermet, E. Wintermantel, Glass–ceramics from municipal incinerator fly ash, *Ceram. Bull.* 76 (11) (1997) 75–78.
- [40] L. Barbieri, A. Corradi, I. Lancellotti, Bulk and sintered glass–ceramics by recycling municipal incinerator bottom ash, *J. Eur. Ceram. Soc.* 20 (10) (2000) 637–1643.
- [41] K.-S. Wang, K.-Y. Chiang, J.-K. Perng, C.-J. Sun, The characteristics study on sintering of municipal solid waste incinerator ashes, *J. Hazard. Mater.* 59 (1998) 201–210.
- [42] M. Romero, R.D. Rawlings, J.M. Rincón, Development of a new glass–ceramic by means of controlled vitrification and crystallization of inorganic wastes from urban incineration, *J. Eur. Ceram. Soc.* 19 (1999) 2049–2058.